A Satellite Radio Interface for IMT-2000

Kwangjae Lim, Kwonhue Choi, Kunseok Kang, Sooyoung Kim, and Ho-Jin Lee

This paper presents a new satellite radio interface, satellite code division multiple access (SAT-CDMA), for the satellite component of IMT-2000. The SAT-CDMA was proposed by Korea and was based on wideband CDMA (WCDMA) for a high degree of commonality with the terrestrial component of IMT-2000. Because a satellite link has a longer round trip delay and a higher Doppler shift than a terrestrial link, we developed new technologies that would make the satellite component especially efficient. We present the main features of the SAT-CDMA radio interface by focusing on satellite-specific schemes. We also demonstrate with extensive comparison results the performance of the main technologies in the SAT-CDMA radio interface.

Manuscript received Mar. 19, 2002; revised Aug. 27, 2002.

This work was supported in part by the Korean Ministry of Information and Communication.

Kwangjae Lim (phone: +82 42 860 6523, e-mail: kjlim@etri.re.kr), Kwonhue Choi (e-mail: khchoi@etri.re.kr), Kunseok Kang (e-mail: kangs@etri.re.kr), Sooyoung Kim (e-mail: sookim@ etri.re.kr), and Ho-Jin Lee (e-mail: hjlee@ etri.re.kr) are with Radio & Broadcasting Research Laboratory, ETRI, Daejeon, Korea.

I. INTRODUCTION

One of the main objectives of IMT-2000 systems is to provide a wide range of services over a wide range of user densities and geographic coverage areas [1]. This feature can best be realized by incorporating both terrestrial and satellite components. The satellite component is attractive for land mobile services over rural and low-population areas and aeronautical and maritime mobile services, as well as for rapid deployment in developing countries. One of the key features of IMT-2000 is a high degree of design commonality and service compatibility in radio specifications of the two components [2].

The main feature in satellite systems that is not in terrestrial systems is a long propagation delay. Kim Shin et al. studied adaptive rain-attenuation compensation schemes [3], and Jang studied a call admission control scheme [4] considering the long delay in the satellite links. The radio transmission technology proposed by Korea, satellite code division multiple access (SAT-CDMA), was approved as a satellite radio interface in an ITU-R recommendation [5] in 1999. As an on-going work, it was updated according to Korean proposals in 2000 and 2001. The SAT-CDMA has a high degree of commonality with the terrestrial radio specification, IMT-2000 Direct Spread (DS), but it also has a number of different features. Those features, which are necessary to reflect the satellite-specific characteristics, such as long round trip delay and high Doppler shift, are implemented in the form of downlink synchronization, uplink packet access, and closed-loop power control. Dealing with the main features of the SAT-CDMA, we present our newly developed schemes and demonstrate their performance.

In section II, we will briefly describe the radio interface of the SAT-CDMA and explain the key technologies. In section III, we demonstrate their simulation results. Finally, conclusions are drawn in section IV.

II. SAT-CDMA RADIO INTERFACE

In this paper, we mainly describe the SAT-CDMA specialized parts because the SAT-CDMA has many similarities with the terrestrial radio interface. Starting from an overall description of the SAT-CDMA physical channels, we will describe the structure of the satellite specialized channels, including downlink synchronization channels (SCH) and dedicated physical channels (DPCH). We then propose a new uplink access scheme for packet service and a novel closed-loop power control scheme.

1. SAT-CDMA Physical Channels

The SAT-CDMA was originally devised to provide mobile satellite services with a maximum data rate of 144 kbit/s, using a satellite constellation of 48 satellites in low earth orbit (LEO) at an altitude of about 1600 km. However, the radio interface of the SAT-CDMA has been developed so that it can be used in various LEO systems with altitudes ranging from 700 km to 1700 km. The SAT-CDMA can also provide a service rate of up to 2 Mbit/s if the link condition is good and a powerful terminal with a large antenna gain is used.

The satellite radio access network (S-RAN) provides a user terminal with diverse IMT-2000 services linked to a terrestrial core network through the SAT-CDMA radio interface. Table 1 shows the key characteristics of the physical layer in the SAT-CDMA radio interface, which are identical to those of the terrestrial IMT-2000 DS for commonality. The SAT-CDMA defines the physical channels similar to those of the terrestrial interface. Table 2 shows the physical channels in IMT-2000 DS and SAT-CDMA. There are several physical channels with a different structure from those of the terrestrial interface and the new defined channel for the SAT-CDMA radio interface. The difference in physical channels stems from the distinct satellite link characteristics from the terrestrial link.

2. Downlink Synchronization Channel

The synchronization channel (SCH) is a downlink channel used for satellite beam search. During the beam search, the user equipment (UE) searches for a beam and determines the downlink scrambling code and frame synchronization for the beam. The SCH consists of two sub-channels—the primary SCH and the secondary SCH—in order to support a hierarchical beam search and thus reduce the beam search time. In the primary SCH, the primary synchronization code (PSC) with a length of 256 chips is repeatedly transmitted once every slot, as shown in Fig. 1. In the secondary SCH, a sequence of 15 secondary synchronization codes (SSCs) is repeatedly transmitted over a frame. The SSC has a length of 256 chips and is transmitted in parallel with the primary SCH.

The hierarchical beam search is based on the same idea as the terrestrial interface, but the synchronization codes transmitted through SCHs are different. Because of a satellite's

Table 1. Key characteristics of SAT-CDMA radio interface.

Access scheme	Direct Spread CDMA
Duplexing	Frequency Division Duplexing
Chip rate	3.84 Mchip/s
Radio frame length	10 ms
Scrambling	Complex scrambling code
Channelization	Orthogonal Variable Spreading Factor (Walsh code)
Modulation	Dual-channel QPSK (for uplink) QPSK (for downlink)

Table 2. Physical channels in IMT-2000 DS and SAT-CDMA.

	IMT-2000 DS	SAT-CDMA
Downlink common	SCH CPICH P-CCPCH S-CCPCH PDSCH PICH AICH AP-AICH CD/CA-ICH CSICH	SCH* CPICH P-CCPCH S-CCPCH PDSCH PICH AICH* AP/CD/CA-ICH* CSICH CPCH-CCPCH+
Downlink dedicated	DPCCH DPDCH	DPCCH* DPDCH
Uplink common	PRACH PCPCH	PRACH* PCPCH*
Uplink dedicated	DPCCH DPDCH	DPCCH* DPDCH

* and + denote the modified channel and the new defined channel, respectively.

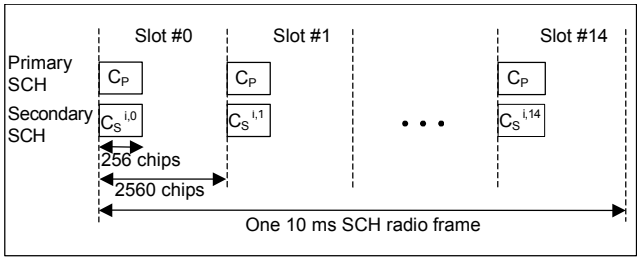

Fig. 1. Structure of the SCH.

fast movement, the Doppler shift reaches several tens of kHz. Although a pre-compensation scheme is applied for each beam, the frequency offset may reach to about 10 kHz because of frequency uncertainty in user terminals as well as the residual Doppler shift after pre-compensation [6]. This prohibits coherent correlation [7] on the synchronization code with a length of 256 chips, because the phase offset may not remain constant within the correlation length (or within 256 chips). The coherent correlation length must be decreased to 128 chips so that the detection performance does not deteriorate (Fig. 2). In the code detection, two 128-chip correlation values are obtained over the synchronization code of the whole 256-chip length, and these values are non-coherently combined. Figure 2 shows the detection performance for a 256-chip code according to various correlation lengths and the number of non-coherently combined values.

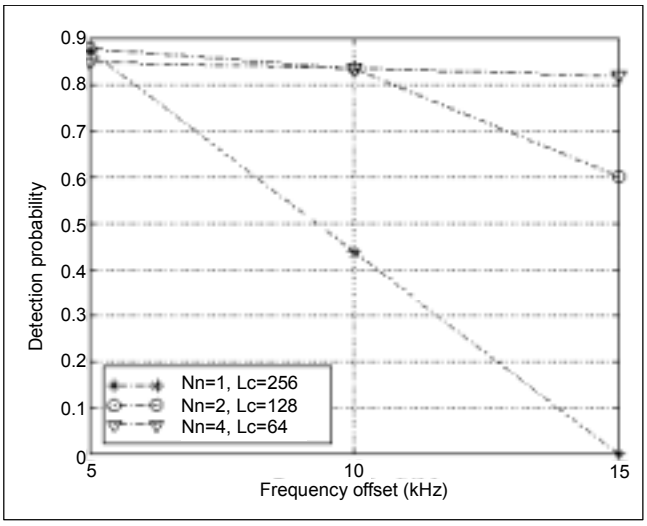

Fig. 2. Detection probability on the primary synchronization code with a 256-chip length (Lc: the coherent correlation length in chips, Nn: the number of non-coherently combined values).

The PSC for the terrestrial interface can be used in the satellite interface without any modifications by using a 128-chip coherent correlation length. However, for the SSC in the satellite interface, it is difficult to use the same code as that used in the terrestrial interface. This is because the SSC includes a Hadamard sequence with a 256-chip length that requires the coherent correlation during the whole code length. Therefore, we need to design a new SSC for the SAT-CDMA. In addition to the need for a new secondary code, a revised primary code is also required in order to minimize cross-correlation between the two codes.

We designed two synchronization codes using hierarchical Golay complementary sequences [8]. The best PSC and SSC were selected from extensive simulations on detection performance.

In the SAT-CDMA, the PSC with a 256-chip length, C_{PSC}, is constructed by the concatenation of two generalized hierarchical Golay sequences, C_{P1} and C_{P2}, each of which has a 128-chip length. The C_{P1} and C_{P2} are obtained by the hierarchical construction of a basis Golay code with an 8-chip length, α_1 and α_2, and a constituent Golay code with a 16-chip length, a_1 and a_2, respectively.

The SSC, C_S, with a 256-chip length is obtained by the hierarchical construction of a basis Golay code with a 16-chip length, β, and a constituent Golay code with a 16-chip length, b_1 and b_2. The b_1 and b_2 are obtained by inverting the sign of 8 chips in the last part of a_1 and a_2, respectively. Therefore, the PSC and the SSC are generalized Golay complementary sequences of each other. In order to generate different secondary codes, the SSC is position-wise multiplied by a Hadamard code with a 256-chip length,

$$C_S^k = < C_{S,1} \times h_{m,1}, C_{S,2} \times h_{m,2}, \ldots, C_{S,256} \times h_{m,256} >,$$

where the Hadamard code h_m, is the m-th row of the following Hadamard matrix $\mathbf{H}_8$:

$$\mathbf{H}_k = \begin{bmatrix} \mathbf{H}_{k-1} & \mathbf{H}_{k-1} \\ \mathbf{H}_{k-1} & \overline{\mathbf{H}}_{k-1} \end{bmatrix}, \; k \geq 1 \quad \text{and} \quad \mathbf{H}_0 = [1].$$

The code of the m-th row, where $m = 8 \times (k-1)$ for k=1,2,…, 16, has the following properties. First, every chip in a segment has the same value as either 1 or –1 when the code is divided into 32 segments and each segment consists of 8 chips. Second, the first part of 128 chips in the code is identical to the last part of the 128 chips. Using these properties, the user terminal can combine each 8-chip segment of the SSC irrespective of the multiplied Hadamard code and coherently detect each 128-chip part of the SSC.

3. Dedicated Physical Channels

In the SAT-CDMA, the dedicated physical channel (DPCH) consists of two sub-channels: the dedicated physical control channel (DPCCH) for physical control information and the dedicated physical data channel (DPDCH) for higher-layer data transmission. For the uplink, the DPCCH and DPDCH are multiplexed in an in-phase channel and a quadrature channel (Fig. 3). For the downlink, the two channels are time multiplexed (Fig. 4). In both links, each frame with a length of 10 ms is split into 15 slots, each with a length 2560 chips.

The DPCCH is used to carry control information generated at the physical layer. The control information consists of known pilot bits for supporting channel estimation for coherent

detection, the transmit power-control (TPC) command, the transport-format combination indicator (TFCI), and feedback information (FBI). The TFCI field is used to inform the receiver about the multiplexing of the higher-layer channels mapped to the DPDCH in the same radio frame.

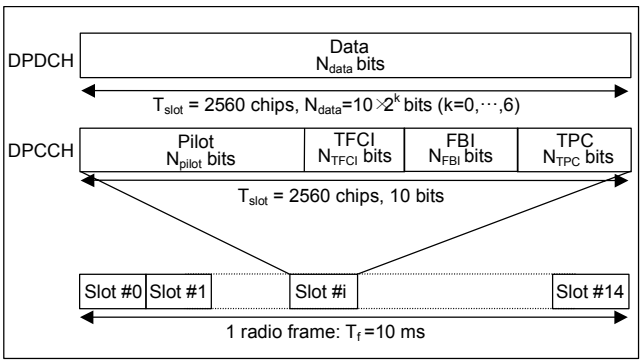

Fig. 3. Frame structure of the uplink DPCH.

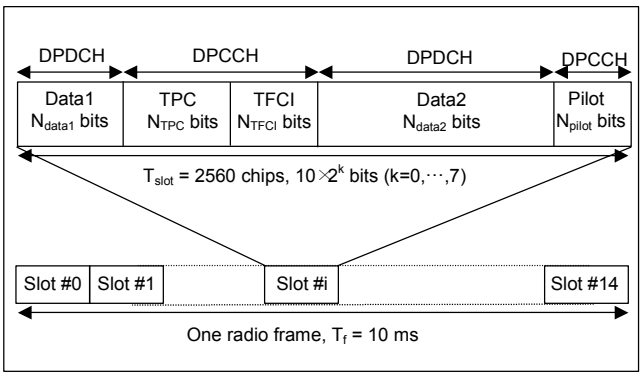

Fig. 4. Frame structure of the downlink DPCH.

In the terrestrial interface, the DPCH supports the fast closed-loop power control in a 1.5 kHz control speed to combat fast fading, such as Rayleigh fading. A TPC command is carried in each slot in a radio frame. However, in a satellite system, the round trip delay between a user terminal and an S-RAN reaches about 10 to 50 ms; these delay values exceed the typical correlation time (less than 10 ms) of a fast fading signal. This suggests that the fast power control for combating fast fading in the terrestrial counterpart is impossible to implement in satellite systems and that we need a different approach to prevent an undesirable increase of interference and power consumption. In the SAT-CDMA interface, a TPC command is transferred once a frame and thus the command rate is 100 Hz. The TPC command consists of two bits defined by the power control procedure described in section II. 6 and is encoded into a codeword by repetition. The code word is then mapped to the TPC fields of 15 slots in a radio frame.

The FBI field is used only in the uplink DPCCH in order to support beam selection diversity transmission (BSDT). In the terrestrial interface, the FBI bits are used when closed-loop transmission diversity is applied in the downlink and the base station transmits signals using two antennas. Additionally, the FBI bits are also used when the site selection diversity TPC (SSDT) as a special case of soft handoff is applied in the downlink. In the SSDT mode a base station, selected as a primary station by a user terminal, transmits the DPDCH and the DPCCH, while others transmit only the DPCCH to maintain a physical link to the user terminal.

In satellite systems, we cannot expect a diversity gain from the spatial separation of two satellite antennas. However, when more than two satellites are involved in a soft handoff, it is possible to achieve the diversity gain from weakly correlated paths from different satellites. In this case, the BSDT is useful to reduce downlink interference. In satellite systems, moreover, a large portion of the beam coverage overlaps and thus the simultaneous transmission by multiple satellites may cause more serious interference.

4. Uplink Random Access

One of the main IMT-2000 services is a packet service. In a radio interface, though both dedicated channels and common channels can be used to carry packet data, the common channel shared by users is efficient for bursty transmission. Like the terrestrial interface, the SAT-CDMA defines two types of physical channels to support the bursty transmission in an uplink: a physical random access channel (PRACH) and a physical common packet channel (PCPCH). The PRACH is used to transmit a short packet over one or two frames without the establishment of a prior radio link. The PCPCH is used to transmit a relatively longer packet over a few tens of frames at most. Although the notation and purpose of these channels are the same in both satellite and terrestrial interfaces, we designed a different operation and procedure for the SAT-CDMA, considering a longer round trip delay [9].

In the random access of the terrestrial interface, a user terminal transmits a preamble and receives a detection indication from a RAN before transmitting the data message. The access scheme using a transmission-after-detection-indication causes a severe access delay in the satellite link because of the long round trip delay. In the SAT-CDMA, the user terminal successively transmits the message along with the preamble, and then it waits for a detection indication for successful reception. The physical layer of an S-RAN immediately transmits the indication without latency for signaling and processing in higher layers. This detection-indication-after-transmission scheme can reduce the access delay more than the transmission-after-detection-indication

scheme. Because of fast acknowledgement, it also has a shorter retransmission delay than the conventional random access scheme. In the conventional scheme, the response message is not a detection acknowledgement of the RAN physical layer but a higher-layer acknowledgement. The higher-layer acknowledgement cannot be transmitted by the S-RAN within the signaling and processing delay in the higher layers, which depends on the content of the random access message.

Figure 5 shows the structure of the random access transmission in the SAT-CDMA interface. The transmission timing is based on the access frame. Each access frame has a length of two radio frames (i.e., 20 ms) and consists of two sub-access frames: an even sub-access frame and an odd sub-access frame (Fig. 6). The use of sub-access frames is optional. When the sub-access frames are used, the user terminal can start the random access transmission at the beginning of either the even sub-access frame or the odd sub-access frame. The random access transmissions at the even sub-access frame and at the odd sub-access frame use different scrambling codes for discrimination.

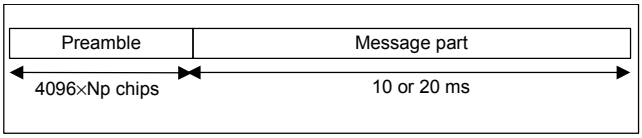

Fig. 5. Structure of the random access transmission.

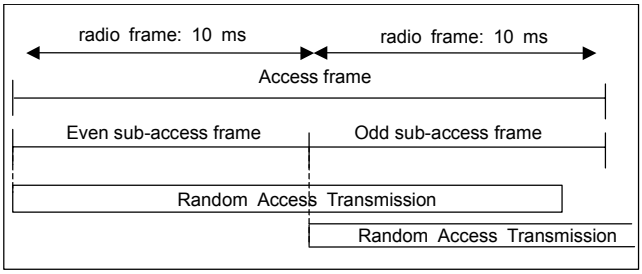

Fig. 6. Access frames.

The random access transmission consists of a preamble with a length of $N_p \times 4096$ chips and a message with a length of 10 ms or 20 ms. The structure of each sub-preamble is identical to that of the preamble in the random access transmission of the terrestrial interface and consists of 256 repetitions of a signature with a length of 16 chips. Every sub-preamble has an identical length and signature code. The same scrambling code sequence with a length of 4096 chips is repeatedly used in the sub-preambles except for the last sub-preamble. The last sub-preamble is scrambled by a conjugate code sequence with a length of 4096 chips. This indicates the end of the sub-preamble repetition. The structure of the message part is identical to that of the terrestrial interface.

The AICH is a downlink channel used for carrying acquisition indicators (AIs). The S-RAN physical layer acknowledges a user's random access by transmitting the AI, which corresponds to the signature used for the preamble transmission on the PRACH. Figure 7 illustrates the structure of the AICH. The AICH access frame has the same length as the PRACH access frame and consists of 15 access slots (AS). The transmission of an AI in the access slot is identical to that of the terrestrial interface. However, in the SAT-CDMA, the AI for the PRACH is transmitted only on the 1st access slot (AS #0) and the 9th access slot (AS #8) at each AICH access frame, but not transmitted during the rest of the 13 access slots. The AI at the 1st access slot corresponds to the signature of the PRACH preamble transmitted at the even sub-access frame, while the AI of the 9th access slot corresponds to that at the odd sub-access frame.

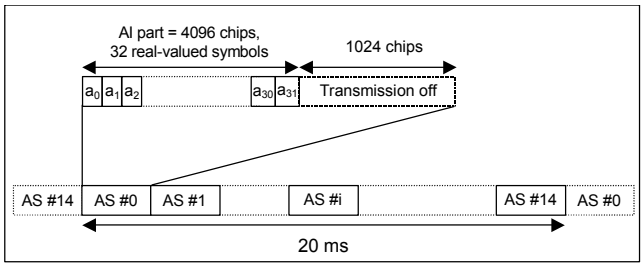

Fig. 7. Structure of the AICH.

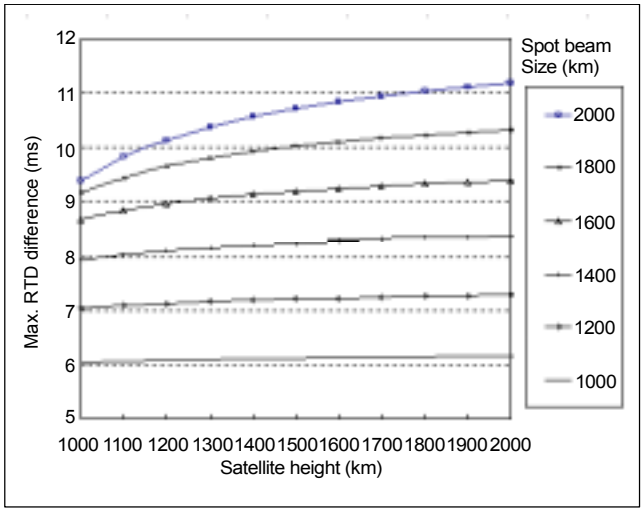

Fig. 8. Difference between the maximum and minimum round trip delays in the satellite spot beam (minimum elevation angle of 15°).

The SAT-CDMA has been designed for a LEO constellation with a satellite altitude of about 700 km to 1700 km. Figure 8 shows the difference between the maximum and minimum

round trip delays for various spot beam sizes. It shows that the delay difference ranges from 6 ms to 12 ms according to satellite altitude and spot beam size. This implies that the transmission interval in an AICH and a PRACH should be longer than a radio frame size of 10 ms. Therefore, in the SAT-CDMA, the access frame of the PRACH and the AICH, which implies a transmission period of the acquisition indicator and the PRACH transmission, has a length of 20 ms.

The downlink AICH frames are time aligned with the primary common control physical channel (P-CCPCH) frame. The uplink PRACH access frame is also time aligned with the received downlink frame. Figure 9 illustrates the PRACH/AICH timing relation. The transmission offset τ_{off} is a value between the range of $[-\tau_{off,max}, \tau_{off,max}]$, defined by the maximum transmission offset $\tau_{off,max}$. The preamble-to-preamble distance $\tau_{p\text{-}p}$ is larger than or equal to the minimum preamble-to-preamble distance $\tau_{p\text{-}p,min}$. The $\tau_{p\text{-}p,min}$ is represented in Table 3 along with the preamble-to-AI distance $\tau_{p\text{-}a}$. The preamble-to-AI distance is closely related to the round trip delay in a satellite spot beam. When the satellite is non-regenerative and the physical layer function is located at a gateway station, the round trip delay has a wide range of about 10 ms to 50 ms according to the location of the spot beam. To deal with the wide range of round trip delay, the SAT-CDMA defines two types of timing parameters as shown in Table 3. When the physical layer function is located at the satellite, the round trip delay is reduced by half. However, the minimum preamble-to-AI distance is taken to be longer than two access frames in consideration of the PRACH transmission length and the processing time at the user terminal and the S-RAN.

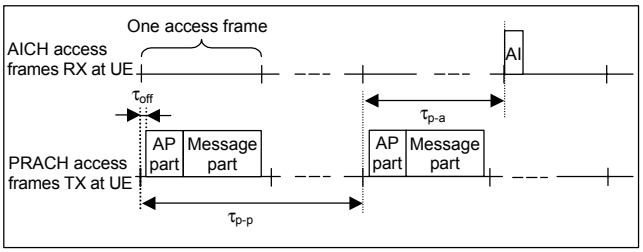

Fig. 9. Timing relation between PRACH and AICH at the user terminal.

Table 3. PRACH/AICH timing parameters according to AICH timing parameter.

AICH timing parameter	$\tau_{p\text{-}p,min}$	$\tau_{p\text{-}a}$
0	3 access frames	2 access frames
1	4 access frames	3 access frames

5. Uplink Packet Access

The PCPCH is intended to carry bursty packets of user data with a length of several tens of frames, while the PRACH is used to transmit a short packet over one or two frames. Therefore, unlike the PRACH, the closed-loop power control is used for the PCPCH. The power control speed is the same, 100 Hz, as for the DPCH.

In the SAT-CDMA interface, we designed a modified uplink packet access scheme so that the PCPCH can be efficiently used for a satellite link with a relatively longer round trip delay. The main elements that are different from the terrestrial counterpart can be summarized as follows: one-step access/channel assignment, the use of a downlink common control channel for PCPCH transmission and power control, and a power control speed of 100 Hz.

In the terrestrial interface, a user terminal transmits an access preamble (AP) as it does the PRACH preamble. After the user terminal receives a positive acknowledgement from the RAN, it transmits a collision detection preamble (CDP). The user terminal cannot acquire permission to access a PCPCH until it receives a positive acknowledgement from the RAN corresponding to the last CDP. This two-step access is inappropriate to satellite systems because it requires at least two times the round trip delay.

In the SAT-CDMA, a user transmits a combined preamble to obtain an access grant. The combined preamble consists of an AP and a CDP, both of which have the same structures as those of the terrestrial counterparts. The S-RAN responds to the preamble, transmitting two consecutive acknowledgements. The user terminal, thus, can obtain transmission permission and channel assignment by a one-step access mechanism.

In the terrestrial interface, an uplink PCPCH is associated with a downlink dedicated control channel. The dedicated channel carries the power control commands and CPCH control commands for the associated PCPCH message transmission. The transmission powers of both channels are controlled by power control commands included in every slot on each channel. However, in a satellite link, the power control period of a slot is inefficient because of a long round trip delay that is much larger than the slot length.

In the SAT-CDMA, the power control period was designed to be equal to a radio frame length. In order to control the transmission and power on the uplink PCPCH, the SAT-CDMA defines a downlink CPCH common control physical channel (CPCH-CCPCH). Up to 15 CPCHs in a CPCH set are associated with the common control channel. Unlike in the terrestrial interface, the transmission power of the downlink channel is not controlled by each PCPCH. Additionally, by

using a common control channel instead of several dedicated control channels, the number of channelization codes available for the downlink can be reduced.

In the SAT-CDMA, the PCPCH transmission is based on a reservation approach. The user can start transmission at the beginning of access frames or sub-access frames. The access frame timing and structure is identical to the PRACH. The structure of the PCPCH access transmission is shown in Fig. 10. The PCPCH access transmission consists of one or several pairs of AP with a length of $N_p \times$ 4096 chips, a CDP with a length of 4096 chips, an initial transmission preamble (ITP) with a length of L_{itp} slots, and a message with a variable length $N \times 10$ ms.

The structure of an AP is identical to that of the PRACH preamble part. Similar to the RACH preamble part, the signature sequences are used in the AP and CDP. The ITP is useful in the demodulation of the message part even for the separation of the preamble and the message part. The structure of the PCPCH message part is identical to that of the PRACH message part. Each message consists of tens of 10 ms frames. A radio frame corresponds to one power-control period. The transmission power of each frame in the message part is controlled by the power control command received on the downlink CPCH-CCPCH.

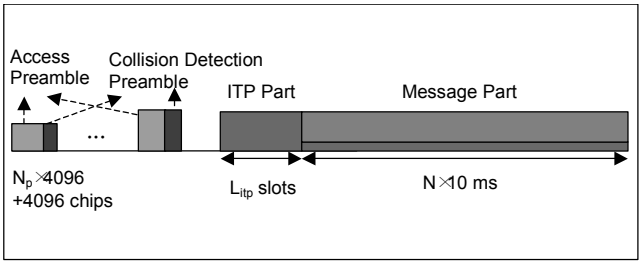

Fig. 10. Structure of the PCPCH transmission.

The access preamble acquisition/collision detection/channel assignment indicator channel (APA/CD/CA-ICH) is a downlink channel used to carry several groups, each consisting of an AP acquisition indicator (API), a collision detection indicator (CDI), and a channel assignment indicator (CAI). The API and CDI correspond to the signatures used in the AP and CDP of the uplink PCPCH, respectively. The CAI indicates a PCPCH channel assigned by the S-RAN. The structure of the APA/CD/CA-ICH is similar to the AICH shown in Fig. 7. However, the APA/CD/CA-ICH is not transmitted on the 1st and 9th access slots. On the rest of the access slots at each AICH frame, several (up to seven) pairs of APIs and CDI/CAIs are transmitted. A pair of an API and a CDI/CAI is transmitted on two consecutive access slots except for the 1st and 9th access slots.

The CCPCH for the CPCH is a fixed rate (30 kbps) downlink channel used to control the uplink PCPCHs in a CPCH set. Figure 11 shows the frame structure of the CPCH-CCPCH. Each slot in the radio frame of the CPCH-CCPCH is associated with the uplink PCPCH. There is a one to one mapping between slot i and PCPCH i in the CPCH set, i=0, 1,…, 14. The slot is not transmitted if the associated PCPCH is not used on the uplink. Each slot consists of a transmit power control (TPC) field with a length of 8 bits and a CPCH control command (CCC) field with a length of 12 bits. The CCC field is used for the transmission of the CPCH control command. The pair of the TPC and CCC in a slot provides the power and transmission control commands for the associated PCPCH.

The downlink APA/CD/CA-ICH frames are time aligned with the P-CCPCH and the uplink PCPCH access frame is time aligned with the reception of the downlink frame as with the PRACH. Figure 12 illustrates the PCPCH/AICH timing relation. The timing relation between the AP/CDP and the APA/CD/CA-ICH is identical to that between the PRACH preamble and the AICH. The timing parameter for the PCPCH is identical to the AICH timing parameter. In addition to $\tau_{p\text{-}p,min}$ and the preamble-to-AI distance $\tau_{p\text{-}a}$ for the PRACH timing parameters, the preamble-to-ITP distance $\tau_{p\text{-}itp}$ is defined as shown in Table 4.

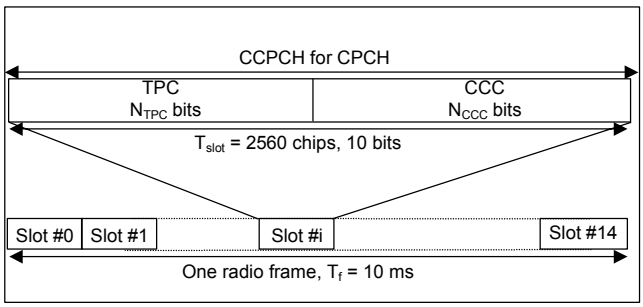

Fig. 11. Frame structure of the CPCH-CCPCH.

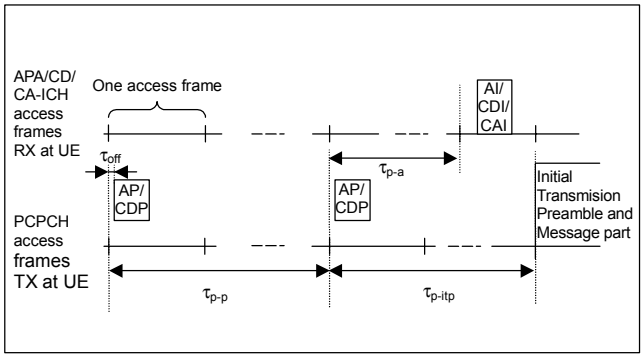

Fig. 12. Timing relation between PCPCH and AICH at the user terminal.

Table 4. PCPCH/AICH timing parameters according to the AICH timing parameter.

AICH parameter	$\tau_{p\text{-}p,min}$	$\tau_{p\text{-}a}$	$\tau_{p\text{-}itp}$
0	3 access frames	2 access frames	3 access frames
1	4 access frames	3 access frames	4 access frames

6. Closed-Loop Power Control

In this section, we describe the uplink/downlink closed-loop power control algorithm employed in the dedicated channel and the uplink packet access channel.

One of the main differences between terrestrial and satellite networks is in a significant difference of the round trip delay. This induces significant degradation of the closed-loop power control if the power control used for the terrestrial interface is employed as it is. In order to reduce the power control error due to such a long delay, two factors should be considered. One is to optimize the basic power control loop parameters, including the power control rate, power control step size, and the number of control levels, because they are highly dependent on the round trip delay and should thus be different from those for the terrestrial interface. The other one is to consider the round trip delay compensation algorithm [10]-[12].

For the case of the uplink closed-loop power control, the UE calculates the actual amount of the transmission power control by using the two most recently received power control commands, which is aimed to change the loop dynamics and shorten the latency in updating transmission power. For the case of the downlink closed power control, the UE may employ a prediction algorithm that estimates the future signal-to-interference ratio (SIR) value after a round trip delay by observing the SIR of the downlink Common Pilot Channel (CPICH). The power control command is generated on the basis of the predicted SIR value.

A. Uplink Closed-Loop Power Control

Figure 13 shows the block diagram of the uplink closed power control loop for the SAT-CDMA. In the uplink closed loop, power control adjusts the UE transmit power in order to keep the received uplink power SIR at a given SIR target, SIR_{target}.

The S-RAN estimates the SIR of the received uplink DPCCH, then generates two-bit TPC commands and transmits the commands once per 10 ms (the length of a radio frame) according to the following rule:

Define $\Delta = SIR_{est} - SIR_{target}$, where SIR_{est} denotes the estimated SIR of the received uplink DPCCH, then a four-level quantized power control step $\Delta_p(i)$ is generated according to the region of Δ:

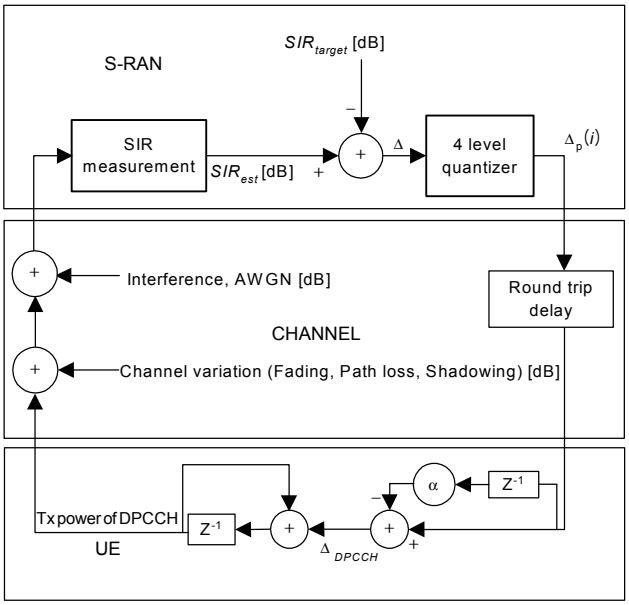

Fig. 13. The block diagram for the uplink closed power control loop.

Table 5. Relationship between $\Delta_p(i)$ and TPC_{cmd}.

TPC_{cmd}	$\Delta_p(i)$
– 2	$-\Delta_L$
– 1	$-\Delta_S$
1	Δ_S
2	Δ_L

$$\text{if} \quad |\Delta| < \varepsilon_T \text{ and } \Delta < 0, \ \Delta_p(i) = \Delta_S,$$
$$\text{if} \quad |\Delta| > \varepsilon_T \text{ and } \Delta > 0, \ \Delta_p(i) = -\Delta_S,$$
$$\text{if} \quad |\Delta| > \varepsilon_T \text{ and } \Delta < 0, \ \Delta_p(i) = \Delta_L,$$
$$\text{if} \quad |\Delta| > \varepsilon_T \text{ and } \Delta > 0, \ \Delta_p(i) = -\Delta_L.$$

The relationship between $\Delta_p(i)$ and the transmitter power control command TPC_{cmd} is presented in Table 5.

Because of the round trip delay, the UE can reflect $\Delta_p(i)$ at its transmission power after about 10 ms to 50 ms during which there may be a considerable change in the SIR. In the SAT-CDMA, we employ a simple preprocessing for $\Delta_p(i)$ before it is reflected at the transmission power in order to compensate for the round trip delay. The UE adjusts the

transmit power of the uplink DPCCH with an amount of Δ_{DPCCH} using the two most recently received power control steps, $\Delta_p(i)$ and $\Delta_p(i-1)$, as follows:

$$\Delta_{DPCCH} = \Delta_p(i) - \alpha\Delta_p(i-1).$$

We can rewrite the above equation as follows:

$$\Delta_{DPCCH} = (1-\alpha)\Delta_p(i) + \alpha(\Delta_p(i) - \Delta_p(i-1)),$$

which means that Δ_{DPCCH} is determined not only by $\Delta_p(i)$ but also by the difference between $\Delta_p(i)$ and $\Delta_p(i-1)$ with weighting factors $(1-\alpha)$ and α, respectively. As α increases, Δ_{DPCCH} becomes more dependent upon the term $\Delta_p(i) - \Delta_p(i-1)$, which corresponds to an estimate for the amount of the recent channel variation.

B. Downlink Closed-Loop Power Control

For the downlink of the SAT-CDMA, unlike the uplink, there is a common pilot channel, CPICH. Since the CPICH is not power-controlled, the channel variation can be estimated by measuring its received power. Therefore, for the downlink closed power control, UE may employ a prediction algorithm, which estimates the future SIR value after a round trip delay. The prediction of the SIR variation can be implemented by observing the SIR of the CPICH.

Figure 14 shows the block diagram of the downlink closed power control loop for the SAT-CDMA. In order to support the prediction at user terminals, the S-RAN periodically broadcasts the round trip delay at the center of the beam through the downlink P-CCPCH. In the SAT-CDMA interface, a predication algorithm is not specified. The prediction algorithm may not be the same for the different user terminals. When the UE is in soft handover, the UE should observe the SIR of all beams' CPICHs in the active set.

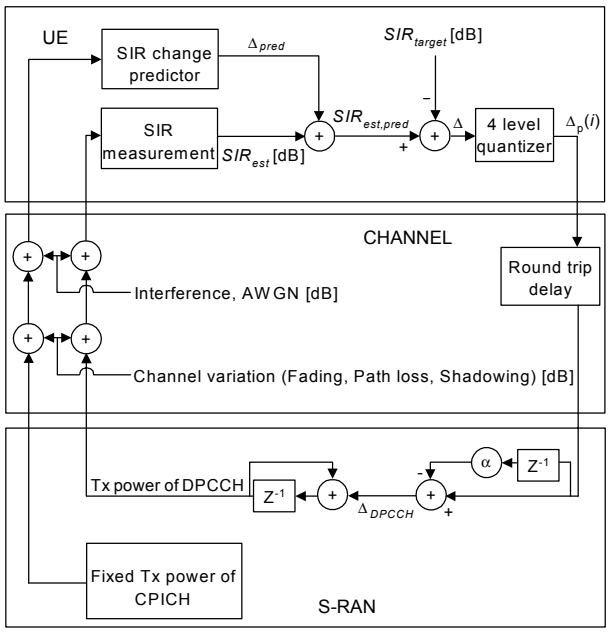

Fig. 14. Block diagram of the downlink closed power control loop.

If the UE predicts the SIR variation after a round trip delay as Δ_{pred}, it is added to SIR_{est} to result in $SIR_{est,pred}$, which is the predicted SIR after the round trip delay as follows:

$$SIR_{est,pred} = SIR_{est} + \Delta_{pred}.$$

The same rule is employed to generate TPC commands as with the uplink closed-loop power control as explained in the previous subsection except that $SIR_{est,pred}$ is used instead of SIR_{est}.

III. SIMULATION RESULTS

In this section, using computer simulations, we present the performance of two key technologies used for the SAT-CDMA interface, the uplink random access for the PRACH transmission and the closed-loop power control for the DPCH and the PCPCH.

1. Uplink Random Access

The physical random access procedure is initiated upon request of the medium access control (MAC) layer. Before the procedure can be initiated, user terminals must receive the RACH-related parameters from the S-RAN and higher layers. Figure 15 describes the whole RACH procedure in the MAC and physical layers at the user side. The MAC RACH procedure can be performed at most $M_{rach,mac}$ times to send a RACH message and the retransmission cycles in the MAC at most $M_{retx,max}$. At the beginning of each retransmission cycle, a persistence test is performed according to a persistence value P_r. After the UE passes the persistence test, it can perform the physical procedure for the PRACH transmission. This persistence test would give an initial delay before the PRACH transmission. In the physical layer procedure, the UE can retransmit up to $M_{ramp,max}$ times, increasing the transmit power, until it receives a correct acknowledgement through the downlink AICH. This acknowledgement indicates the successful reception of the UE's preamble and message.

The S-RAN response on the content in the RACH message is transmitted through the downlink forward access channel (FACH) on the secondary common control physical channel (S-CCPCH). If the UE receives the response message, it stops the RACH procedure at any time during the RACH procedure.

Generally, because of the processing time for the transmission/reception and signaling, it takes hundreds of milliseconds before the S-RAN transmits the response message on the FACH. Therefore, the UE has to wait for the response for a long time with the conventional random access scheme, where there is no fast acknowledgement as with AI on the AICH in the SAT-CDMA.

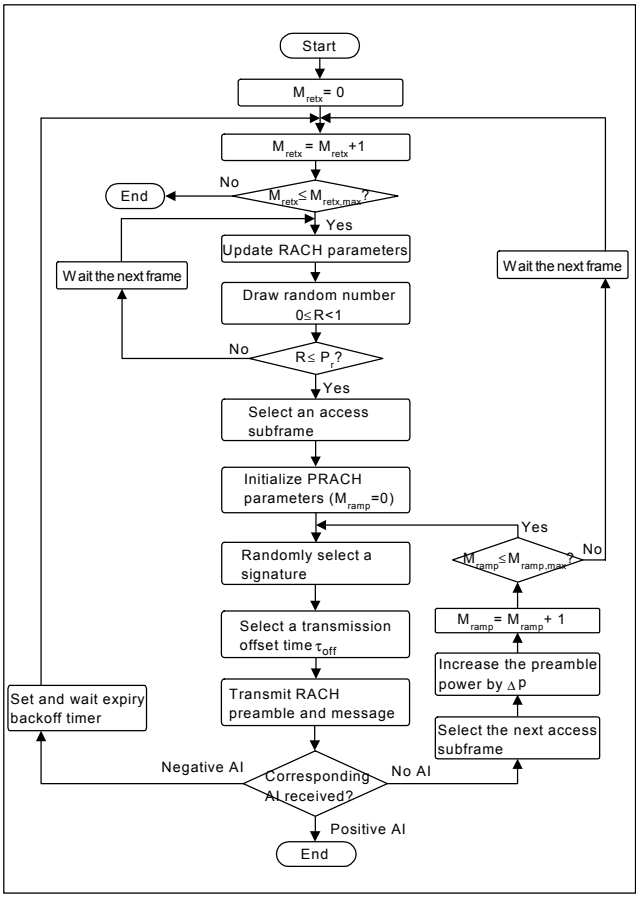

Fig. 15. RACH procedure at the UE.

In the terrestrial interface, the preamble and the message parts are separately transmitted. In this case, the UE must wait for a detection indication corresponding to its preamble during at least one round trip delay and processing time before it transmits the message part. If this scheme is used in the SAT-CDMA, the UE would have to wait for the time period of 6 or 8 frames as described in section II. 4.

We performed simulations to evaluate the performance of random access transmission schemes for the SAT-CDMA and the terrestrial radio interfaces as well as the conventional random access scheme. The performance was evaluated in terms of delay and throughput.

Table 6 shows the simulation environment and parameters. In our simulations, the RACH messages at the UE are generated by a Poisson process with a mean arrival rate. Each UE in a spot beam experiences independent Rician fading and log-normal shadowing [13]. The round trip delay is assumed to be within 39 to 49 ms considering a LEO satellite altitude of 1600 km and an elevation angle of 40 degrees. The initial transmit power of the preamble is estimated by the UE using the open-loop power control. It is assumed that a power control error is generated by a Gaussian distribution with a standard deviation in dB scale [14]. The preamble structure of the conventional and terrestrial schemes is identical to that of the SAT-CDMA scheme. We assume that the preamble and the message can be successfully received if the average received SIR exceeds the required SIR in Table 6.

Table 6. Simulation environment and parameters for the RACH.

RACH message arrival	Poisson process
RACH message length	1 frame
Round trip delay	Uniform over 39 to 49 ms
Open loop power control error	Gaussian with a std of 3 dB
Fading model	Rician and Log-normal fading
Carrier frequency	2 GHz
Elevation angle	40 degree
Mobile speed	3 and 70 km/h
Required SIR for preamble	– 18 dB
Required SIR for message	– 15 dB
Number of RACH trials	3
Number of retransmission cycles	3
Number of power-rampings	3
Persistence value	0.5
Backoff time for the negative AI	Uniform over 1 to 10 frames
Message backoff time	Uniform over 1 to 10 frames
RACH/FACH signaling delay	10 frames
Preamble length	3×4096 chips (N_p= 3)
Number of signatures	16
Transmission offset	0 chip
Preamble-to-preamble distance	8 frames
Preamble-to-AI distance	6 frames
Preamble-to-message distance	8 frames
Power-ramping step size	3 dB

The RACH/FACH signaling delay implies a time duration from the reception of the RACH message to the transmission of the FACH response message at the S-RAN. In the simulation for the conventional scheme, the UE thus waits

during a time period of 18 frames from the time of the PRACH transmission.

Figures 16 and 17 show the simulation results for the throughput and transmission delay when the mobile speed is 3 km/h and 70 km/h, respectively. Terrestrial, conventional, and SAT-CDMA in the legend denote the random access schemes of the terrestrial interface, the conventional system, and the SAT-CDMA interface, respectively. The arrival rate indicates the average number of messages generated in the radio frame duration (10 ms). The throughput indicates the average number of successfully received messages per radio frame, and it was normalized by the target SIR of the message part. The transmission delay indicates the average delay from the message generation time at the UE to the reception time at the S-RAN, and it was scaled by the radio frame duration.

Figure 16 shows that the conventional scheme has the maximum throughput T_{max} at about 0.28, where the arrival rate λ has the same amount. It becomes unstable if λ is larger than 0.28, so that the throughput falls rapidly and the delay increases abruptly. In this situation, the arrival rate exceeds the limit that the conventional scheme can support. For the SAT-CDMA scheme, T_{max} reaches about 0.31, and we can see this is the highest value of the three schemes. We note that T_{max} for the conventional and the terrestrial schemes are 0.28 and 0.18, respectively.

The SAT-CDMA has a smaller delay than the terrestrial by about 10 frames to 30 frames. As mentioned in the previous sub-section, with the terrestrial scheme, the user terminal has to wait for the success of the preamble transmission before the message part is transmitted. Additionally, although the preamble is successfully received at the S-RAN, a successful transmission of the message cannot be guaranteed because the channel and interference situation will change after the time duration of the preamble-to-message distance.

If the probability used for the persistence test is controlled according to the traffic load or the arrival rate, the abrupt drop of the throughput at T_{max} can be avoided. Although such load adaptation can be commonly applicable to the other two schemes, it will not change the throughput-delay performance trends; thus the superior performance of the SAT-CDMA scheme over the other schemes will be sustained.

Figure 17 shows the throughput-delay performance at a mobile speed of 70 km/h. We note that the terrestrial scheme shows almost the same performance as that with a low mobile speed. On the other hand, the conventional and SAT-CDMA schemes show deteriorated performance. This performance difference with the mobile speed results from the preamble and message transmission schemes. In the terrestrial scheme, a preamble and a message are separately transmitted with an interval of at least a round trip delay ($\tau_{p,min}$), and thus the fading and interference situation for the preamble and the message would be different irrespective of the mobile speed. In the conventional and the SAT-CDMA schemes, the fading and interference situation would be highly dependent on the mobile speed. Nevertheless, the SAT-CDMA scheme still shows the best performance even with the high mobile speed.

These simulation results demonstrate that the random access scheme for the SAT-CDMA is superior to the other schemes. Compared with the conventional scheme, the SAT-CDMA

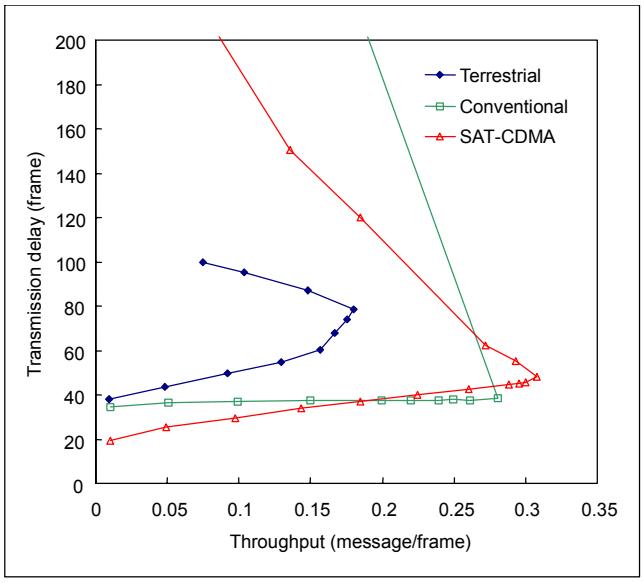

Fig. 16. Throughput-delay performance for random access schemes for a mobile speed of 3 km/h.

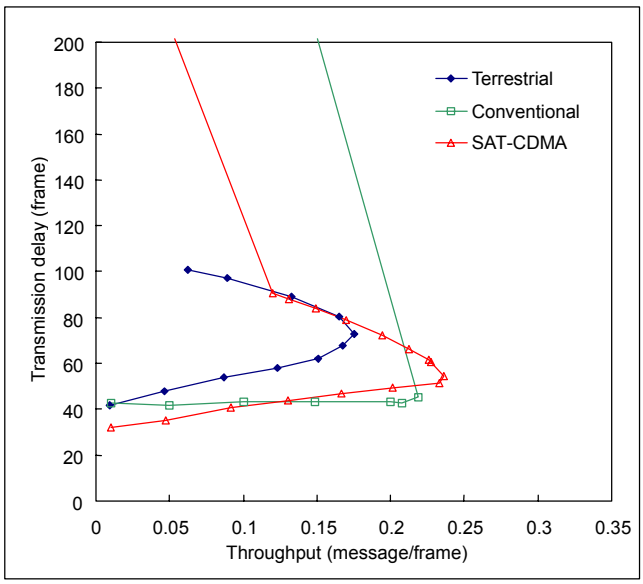

Fig. 17. Throughput-delay performance for random access schemes for a mobile speed of 70 km/h.

scheme has a feature of fast detection acknowledgement that results in a retransmission delay reduction and a throughput increase. On the other hand, compared with the terrestrial scheme, the SAT-CDMA scheme has a feature of one-step transmission that results in a shorter access delay and throughput increase.

2. Closed-Loop Power Control

In order to investigate the performance of the closed-loop power control algorithm, we simulated the power control loop under the simulation parameters given in Table 7. The same channel model as for the random access simulation in section III. 1 was used.

Table 8 shows the performance of the uplink closed-loop power control. The standard deviations of the power control error in log-linear scale are given for the cases when the compensation algorithm is employed and are compared to the case when the Δ_{DPCCH} is simply adjusted to equal $\Delta_p(i)$ as with the terrestrial case.

Table 7. Simulation parameters for the power control procedure.

Parameters	Values
Power control interval	10 ms
SIR averaging window size	10 ms
Mobile speed	3 and 70 km/h
Round trip delay	20 and 50 ms

Table 8. Standard deviations of the uplink power control error.

Round trip delay [ms]	Mobile speed [km/h]	Standard deviation of the power control error [dB] and optimum parameters for (Δ_S, Δ_L) and (Δ_S, Δ_L, α)	
		Case without prediction and delay compensation	Case with prediction and delay compensation
20	3	2.6 (0.7, 1.4)	2.3 (0.6, 1.2, 0.47)
	70	5.8 (0.7, 1.4)	5.6 (0.9, 1.8, 0.23)
50	3	4.9 (0.2, 0.4)	3.7 (0.2, 0.4, 0.85)
	70	7.3 (0.4, 0.8)	6.7 (0.3, 0.6, 0.82)

In order to compare the performance under various channel conditions, we considered four combinations for round trip delay and UE speed. For each case, the optimum values for the power control steps Δ_S and Δ_L and the compensation algorithm parameter α are also tabulated in Table 8. It shows that the optimum power control steps Δ_S and Δ_L decrease as the round trip delay increases in order to avoid fluctuation in the loop. On the other hand, the optimum α increases as the round trip delay increases.

The compensation algorithm reduces power control errors regardless of the round trip delay or the UE velocity. Especially, the improvement is the most apparent for the case when the round trip delay is large. This is because, as the round trip delay increases, the amount of the SIR change increases and thus the compensation algorithm is more effective.

The compensation also performs better for a velocity of 3 km/h than for a velocity of 70 km/h. This can be explained by the fact that the prediction for future increments (or decrements) of the SIR by the term $\Delta_p(i) - \Delta_p(i-1)$ becomes less accurate as the mobile speed increases, because the SIR varies faster and thus does not maintain a constant slope during the round trip delay. For a round trip delay of 50 ms and a velocity of 3 km/h, the proposed compensation achieves a reduction of 1.2 dB in power control error.

Table 9 shows the performance of the downlink closed-loop power control where the SIR prediction is employed along with round trip delay compensation as done in the uplink power control. The same simulation parameters as in Table 7 are used. For an SIR change predictor, we employed a simple algorithm where Δ_{pred} is proportional to the amount of change of the CPICH SIR during the last power control period with a gain parameter G as follows:

$$\Delta_{pred} = G(SIR_{CPICH}(i) - SIR_{CPICH}(i-1)),$$

where $SIR_{CPICH}(i)$ is the CPICH SIR for the i-th power control period. We compared the results to those without prediction (G=0) and round trip delay compensation (α=0). For each case, the optimum values for the power control steps Δ_S and Δ_L, the compensation algorithm parameter α and the prediction scale factor G are also given in Table 9. The prediction scale factor G is significant for the case of a small velocity (3 km/h) because the channel variation is slow and thus, the prediction is reliable.

Besides the improvement by round trip delay compensation, an additional improvement can be obtained by using the prediction algorithm. Again, we note that the improvement is the most noticeable for a round trip delay of 50 ms and a velocity of 3 km/h. Comparing the results in Table 6, we find that there is an additional reduction of 0.3 dB in power control error when we add the prediction algorithm for a round trip delay of 50 ms and a velocity of 3 km/h. After all, the SIR prediction along with round trip delay compensation can reduce maximally the power control error by 1.7 dB in total.

Table 9. Standard deviation of the downlink power control error.

Round trip delay [ms]	Mobile speed [km/h]	Standard deviation of the power control error [dB] and optimum parameters for (Δ_S, Δ_L) and (Δ_S, Δ_L , α, G)	
		Case without prediction and delay compensation	Case with prediction and delay compensation
20	3	2.6 (0.7, 1.4)	2.1 (0.6, 1.2, 0.47, 2.0)
	70	5.8 (0.7, 1.4)	5.5 (0.7, 1.4, 0.47, 0.1)
50	3	4.9 (0.2, 0.4)	3.2 (0.3, 0.6, 0.8, 5.0)
	70	7.3 (0.4, 0.8)	6.7 (0.3, 0.6, 0.97, 0.1)

IV. CONCLUSIONS

In this paper, we presented the SAT-CDMA of a satellite radio interface for IMT-2000. We extensively overviewed the SAT-CDMA by comparing it to the terrestrial radio interface and emphasized satellite-specific interfaces. We proposed several efficient techniques for the SAT-CDMA. The distinct techniques include uplink random access, uplink packet access, closed-loop power control, downlink synchronization, and satellite selection diversity. We introduced random access and power control techniques and demonstrated their simulation results on the satellite link. We compared the simulation performances of these schemes to those used for terrestrial radio interface and other systems. In the simulation, the developed power control scheme gave about a 1.7dB reduction in power control error. The developed random access showed about a 170% throughput enhancement and transmission delay reduction, which is the amount comparable to several round trip delays. For third generation mobile services, besides the terrestrial radio access network, the SAT-CDMA will play an important role in the radio access network by virtue of the satellite-specific technologies introduced in this paper as well as the unique broadcast and large coverage capabilities of the satellite system. In addition, the developed technologies, which were designed to be efficient in satellite systems, can be applied to provide the next generation broadband satellite services.

REFERENCES

[1] Recommendation ITU-R M.687-2, *International Mobile Telecommunications-2000*, 1997.

[2] Recommendation ITU-R M.1034-1, *Requirements for the Radio Interface(s) for IMT-2000*, 1997.

[3] Sooyoung Kim Shin, Kwangjae Lim, Kwonhue Choi, and Kunseok Kang, "Rain Attenuation and Doppler Shift Compensation for Satellite Communications," *ETRI J.*, vol. 24, no. 1, Feb. 2002, pp. 31-42.

[4] Yeong Min Jang, "Estimation and Prediction-Based Connection Admission Control in Broadband Satellite Systems," *ETRI J.*, vol. 22, no.4, Dec. 2000, pp. 40-50.

[5] Recommendation ITU-R M.1457 revision 1, *Detailed Specifications of the Radio Interfaces of IMT-2000*, 2001.

[6] Moon-Hee You, Seong-Pal Lee, and Youngyearl Han, "Adaptive Compensation Method Using the Prediction Algorithm for the Doppler Frequency Shift in the LEO Mobile Satellite Communication System," *ETRI J.*, vol. 22, no. 4, Dec. 2000, pp. 32-39.

[7] Yi-Pin Eric Wang and Tony Ottosson, "Cell Search in W-CDMA," *IEEE J. Select. Areas Comm.*, vol. 18, no. 8, Aug. 2000, pp. 1470-1482.

[8] Srdjan Budisin, "Golay Complementary Sequences are Superior to PN Sequences," *Proc. of IEEE Int'l Conf. on Systems Engineering*, Sept. 1992, pp. 101-104.

[9] Kwangjae Lim and Sooyoung Kim Shin, "Uplink Packet Access for SAT-CDMA," *Proc. of CIC*2001, CD-ROM title, 2001.

[10] F.C.M. Lau and W.M. Tam, "Novel SIR-Estimation-Based Power Control in a CDMA Mobile Radio System under Multipath Environment," *IEEE Trans. Veh. Tech.*, vol. 50, no. 1, Jan. 2000, pp. 314-320.

[11] Sangho Choe, T. Chulajata, H.M. Kwon, Byung-Jin Koh, and Sung-Cheol Hong, "Linear prediction at base station for closed loop power control," *Proc. of VTC*1999, vol. 2, 1999, pp. 1469-1473.

[12] M.L. Sim, E. Gunawan, C.B. Soh, and B.H. Soong, "Study on the Characteristics of Predictive Closed-Loop Power Control Algorithms for a Cellular DS/CDMA System," *Proc. of ICUPC*'98. vol. 2, 1998, pp. 981-985.

[13] Michael J. Miller, Branka Vucetic, and Les Berry, *Satellite Communications: Mobile and Fixed Services*, Kluwer Academic Pub., 1993.

[14] Anton M. Monk and Laurence B. Milstein, "Open-Loop Power Control Error in a Land Mobile Satellite System," *IEEE J. Select. Areas Comm.*, vol. 13, no. 2, Feb. 1995, pp. 205-212.

Kwangjae Lim received BS, MS, and PhD degrees in electronics engineering from Inha University, Korea, in 1992, 1994 and 1999. In March 1999, he joined ETRI, Korea, as a Senior Member of Research Staff. Since 1999, he has worked on standardization on IMT-2000 and he is currently charged with the working group on satellites under the project group on IMT-2000 and systems beyond, at Telecommunications Technology Association (TTA), Korea. His research interests are adaptive transmission schemes, medium access control and radio resource allocation in mobile and wireless communication systems.

Kwonhue Choi received the BS, MS, and PhD degrees in electronic and electrical engineering from the Pohang University of Science and Technology (POSTECH), Korea, in 1994, 1996 and 2000. Since 2000, he has been with ETRI, Korea, and has worked for the development of efficient transmission algorithms for satellite communications. His research interests are performance analysis of CDMA networks and demodulation algorithms for digital modems. Currently, he is interested in adaptive transmission algorithms for wideband CDMA systems in the fading environment.

Kunseok Kang received the BS and MS degrees in School of Electronics and Electrical Engineering from Kyungpook National University, Korea, in 1997 and 1999. He is currently a Member of Research Staff at Broadband Wireless Communication Department of ETRI, Korea, and has worked for the development of efficient transmission algorithms for satellite communications. His research interests include satellite communications, coding technique, and multicarrier transmission.

Sooyoung Kim received the BS degree in electrical and electronics engineering from Korea Advanced Institute of Science and Technology, Korea, in 1990. After having worked Satellite Communication Technology Division, ETRI, Korea from February 1990 to September 1991, she received the MSc and the PhD degrees in electrical and electronics engineering from University of Surrey, UK in 1992 and 1995. From November 1994 to June 1996 she was employed as a Research Fellow at the Centre for Satellite Engineering Research, University of Surrey, UK. In 1996 she re-joined the Satellite Communication Technology Division, ETRI, Korea. She is currently a Team Leader of the Broadband Wireless Transmission Team and is responsible for developing efficient adaptive multi-carrier transmission schemes to compensate for channel impairments in satellite communication systems. Her work also includes developing highly efficient coding techniques for digital communication systems.

Ho-Jin Lee received his BS, MS, PhD degrees in electronics engineering from Seoul National University (SNU), Korea, in 1981, 1983 and 1990. He joined ETRI in 1983 and has been involved with TDX, a full electronic digital switching system development project, satellite ground mission/network control system development, KOMPSAT ground control system development, and satellite communication earth stations/service development. He has been with TRW, USA, as a Visiting Engineer for 2 years. He worked as the Director of the Satellite Communications Application Department of ETRI and is now the Project Manager of a DVB-RCS system, two-way satellite broadband access system development project.